CityU
香港城市大學
City University of Hong Kong
專業 創新 胸懷全球
Professional·Creative
For The World

CityU Scholars

# Investigation on hybrid system design of renewable cooling for office building in hot and humid climate

Fong, K.F.; Lee, C.K.

**Published in:**
Energy and Buildings

**Published: 01/06/2014**

**Document Version:**
Post-print, also known as Accepted Author Manuscript, Peer-reviewed or Author Final version

**License:**
CC BY-NC-ND

**Publication record in CityU Scholars:**
Go to record

**Published version (DOI):**
10.1016/j.enbuild.2014.02.004

**Publication details:**
Fong, K. F., & Lee, C. K. (2014). Investigation on hybrid system design of renewable cooling for office building in hot and humid climate. *Energy and Buildings*, *75*, 1-9. Advance online publication. https://doi.org/10.1016/j.enbuild.2014.02.004

**Citing this paper**
Please note that where the full-text provided on CityU Scholars is the Post-print version (also known as Accepted Author Manuscript, Peer-reviewed or Author Final version), it may differ from the Final Published version. When citing, ensure that you check and use the publisher's definitive version for pagination and other details.

**General rights**
Copyright for the publications made accessible via the CityU Scholars portal is retained by the author(s) and/or other copyright owners and it is a condition of accessing these publications that users recognise and abide by the legal requirements associated with these rights. Users may not further distribute the material or use it for any profit-making activity or commercial gain.

**Publisher permission**
Permission for previously published items are in accordance with publisher's copyright policies sourced from the SHERPA RoMEO database. Links to full text versions (either Published or Post-print) are only available if corresponding publishers allow open access.

**Take down policy**
Contact lbscholars@cityu.edu.hk if you believe that this document breaches copyright and provide us with details. We will remove access to the work immediately and investigate your claim.

Download date: 18/04/2024

# Investigation on hybrid system design of renewable cooling for office building in hot and humid climate

K.F. Fong*, C.K. Lee

Division of Building Science and Technology, City University of Hong Kong, Tat Chee Avenue, Kowloon, Hong Kong, China

*Corresponding author.

Tel: 852-3442-8724, fax: 852-3442-9716

Email address: bssquare@cityu.edu.hk

Post address: Tat Chee Avenue, Kowloon, Hong Kong, China

http://dx.doi.org/10.1016/j.enbuild.2014.02.004

**Abstract**

In this study, a hybrid renewable cooling system (HRCS) is proposed for office building application by utilizing both the solar energy and the ground source. With the basis of solar absorption cooling, part of the building sensible cooling load was shared by the ground-source radiant cooling. Although the solar absorption cooling system or the ground source heat pump system has been individually proven energy-efficient, the area of solar collectors or size of borehole field would be limited by the available space for accommodation. In this regard, the system performance through joint contribution of renewable energy sources was investigated for building air-conditioning purpose. In the HRCS, appropriate design and operation between the ground-source radiant cooling and

the solar absorption cooling was worked out. Through year-round dynamic simulation, it was found that the HRCS could have 43.8%, 53.3% and 68.0% primary energy saving when compared to the sole ground-source heat pump system, the sole solar absorption cooling system and the conventional vapour compression air-conditioning system respectively. This demonstrates the merit of hybrid utilization of solar energy and ground source, and the strategy of renewable cooling is robust for sustainable air-conditioning and green building design in hot and humid climate.

*Keywords*: Renewable cooling; hybrid system; solar energy; ground source; air-conditioning.

**Nomenclature**

| | |
|---|---|
| $COP$ | coefficient of performance of chiller |
| $k_g$ | thermal conductivity of the ground ($W \cdot m^{-1} \cdot K^{-1}$) |
| $\dot{q}$ | heat source in the ground ($W \cdot m^{-3}$) |
| $Q_{ab}$ | heat rejected from the absorber (kW) |
| $Q_{cond}$ | heat rejected from the condenser (kW) |
| $Q_{evap}$ | heat absorbed from the evaporator (kW) |
| $Q_{gen}$ | heat injected into the generator (kW) |
| $RH_{zone}$ | zone relative humidity (%) |
| $SF$ | solar fraction |
| $T_g$ | ground temperature ($^oC$) |

| | |
|---|---|
| $T_{zone}$ | zone temperature ($^{o}$C) |
| $t$ | time (s) |
| $\rho c_g$ | volumetric heat capacity of the ground ($J \cdot m^{-3} \cdot K^{-1}$) |

Abbreviation

| | |
|---|---|
| CC | chilled ceiling |
| GHE | ground heat exchanger |
| GHPS | ground-source heat pump system |
| HRCS | hybrid renewable cooling system |
| IEA | International Energy Agency |
| PCB | passive chilled beams |
| SACS | solar absorption cooling system |
| VCCS | vapour compression chiller system |

## 1. Introduction

The International Energy Agency (IEA) has set up the Solar Heating and Cooling Programme to promote the technology development and standardization of solar heating and cooling since 1977 [1]. General design guidelines and demonstration projects have been established to promote wider use of solar heating and cooling [2,3]. In addition, basic design calculations and discussions of solar cooling have been provided for various common solar refrigeration and air-conditioning systems [4,5]. Solar energy systems have been designed for buildings through solar heating and cooling, as well as different integrated methods [6]. In recent years, there is a shift from "solar heating and cooling" to "renewable heating and cooling" by IEA [7], by involving additional renewable energy

sources, like geothermal energy and bioenergy. To align the energy policies of reducing the use of non-sustainable energy sources, the barriers of renewable heating and cooling have been reviewed and its opportunities have been identified [8,9]. Policy guidelines of renewable heating and cooling have also been developed in order to facilitate the research potential and the market penetration in the European level [10].

In the aspect of utilizing solar energy and geothermal energy, Georgiev et al. [11] conducted response test and charging-discharging test to work out borehole thermal energy storage with solar collectors in Chile. By using solar energy and ground-source feature, this study established the technical details of soil properties and predicted the temperature variation along charging/discharging cycle for sake of underground thermal energy storage. Ozgener and Hepbasli [12] made use of solar energy and geothermal energy to develop the solar-assisted ground-source heat pump, which was applied for greenhouse heating in Turkey. Through the experimental setup, its coefficient of performance for heating and exergetic efficiency of the entire system were evaluated. Wang et al. [13] carried out dynamic simulation study of solar-assisted ground-source heat pump in connection to the soil and soil heat exchanging modelling on monthly basis. Since the soil temperature could be predicted to increase annually, it is effective for the system to operate for alternative cooling and heating in long run. Through simulation study, Kim et al. [14] analyzed the component and system performance characteristics of solar-assisted ground-source heat pump, in which a heat storage tank was used to store up thermal energy and supply for residential heating. It was found that the system performance was very sensitive to heat pump operating temperature. Appropriate indoor temperature setting in accordance with the changing outdoor temperatures is important for achieving good system performance of solar-assisted ground-source heat pump for

heating purpose. So far, these studies have mainly emphasized on renewable heating through solar energy and geothermal energy, rather than renewable cooling alone.

In fact, renewable cooling itself is more paramount in the hot and humid cities, where building cooling is indispensable throughout the year and heating is minor in general. Currently, little concrete research outcomes in design strategies of renewable cooling are disseminated. As a result, a hybrid renewable cooling system (HRCS) is proposed for building application in this case study. Solar-thermal air-conditioning system which employs absorption chiller driven by evacuated tube collectors has been found to be the most energy-efficient way for building use in the sub-tropical region [15]. To further reduce the energy consumption, radiant cooling can be adopted to handle part of the zone sensible load, and the operating time for the absorption chiller can be reduced accordingly. A "high-temperature" chilled water supply can be achieved by coupling the radiant panels directly with a ground heat exchanger (GHE) borefield. Through the involvement of solar absorption cooling and ground-source radiant cooling, the HRCS is established through the hybrid use of solar energy and shallow geothermal merit.

The rest of the paper is structured in the following way. Section 2 describes schematic design, model development, control and operation, and parameter details of HRCS. Section 3 states the comparative study with the associated renewable cooling systems and the metrics of performance analysis. Section 4 discusses the results of HRCS and its refinement, also compares the effectiveness among various cooling systems. Section 5 is conclusion and recommendation.

## 2. System development and dynamic modelling of hybrid renewable cooling

### *2.1 Components of HRCS*

Fig. 1 shows the schematic diagram of HRCS. Evacuated tubes are employed as the solar collectors for the absorption chiller. An auxiliary heater is used for the chiller in case the solar thermal gain is not sufficient. The supply air coil is controlled by a proportional controller which monitors the zone temperature. The supply air fan and the chilled water pump run continuously during the entire daily operating period. The regenerative water pump and the cooling water pump are energized when the chiller starts as determined by a return chilled water thermostat. The cooling tower is additionally controlled according to the cooling water temperature leaving the chiller. The operation of the hot water pump, used to convey the solar heat to the hot water storage tank, is governed by a differential thermostat which ensures that the water leaving the solar collector is always higher than that inside the storage tank within the daily operation schedule. Another differential thermostat is used to control the borefield water pump within the daily operation schedule, so that the water temperature leaving the borefield is always lower than the zone temperature. For the radiant panels, both the chilled ceiling (CC) and the passive chilled beams (PCB) are considered in this study. Only temperature-control is offered for the system and both the supply air coil and the ground-source radiant panels will operate when the zone temperature rises above a pre-set upper limit. The proportional controller is used to regulate a supply air coil valve which governs the chilled water flow through the supply air coil. Meanwhile, the radiant cooling system operates in full capacity once it is energized.

*2.2 System model development for dynamic simulation*

Year-round dynamic simulation was carried out to evaluate the system performances in changing building loads and climatic conditions in this study. The component-based simulation platform TRNSYS [16] and its component library TESS [17] were applied. For the building, a typical office zone [18] with floor area of 196 $m^2$ was adopted in this study. The daily operating period was from 8:00 a.m. to 6:00 p.m. The maximum number of occupants was 24, the lighting heat gain was 17 $W/m^2$ and the office equipment power density was 25 $W/m^2$. The constructional characteristics and parameters of typical office building are summarized in Table 1. The design indoor conditions were of 25.5$^oC$ and 60%RH, and the design outdoor conditions were 33.5$^oC$ and 68%RH. The fresh air requirement was 0.01 $m^3/s$ per occupant. The estimated system sensible load and latent load, therefore, were 20 kW and 9 kW respectively. The typical meteorological data for Hong Kong [19] was applied in dynamic simulation, and the key weather information is summarized in Table 2 for reference. For the CC, the built-in active layer specification in the standard multi-zone model (Type56) [20] of TRNSYS was applied. Default parameters adopted in the TRNSYS components were used unless otherwise specified. For the PCB, an empirical model was developed which was based on the catalogue data from the manufacturer [21]. The efficiency coefficients determined by [22] were adopted for the evacuated tubes. The total area of the solar collectors was 100 $m^2$, and the size of the hot water storage tank was 5 $m^3$.

For the ground heat exchanger borefield, a new component model was developed based on the finite volume model of Lee and Lam [23]. Fig. 2 shows the ground discretization scheme employed. Each borehole was represented by a square column

circumscribed by the borehole radius. The heat transfer in the ground was assumed to be purely conductive so that

$$\rho c_g \frac{\partial T_g}{\partial t} = k_g \nabla^2 T_g + \dot{q} \quad (1)$$

Here $\dot{q}$ was the source term which was governed by the convective heat transfer inside each borehole under the prescribed borehole surface temperature profile along each borehole surface which was determined by utilizing respective interference coefficients presented by Hellstrom [24]. The two heat transfer solutions coupled with each other which were solved in an iterative manner at each simulation time step.

Fig. 3 shows the schematic diagram of a single-effect lithium bromide absorption chiller from a previous study [25]. Water vapour was used as the refrigerant which was generated from the generator, passed into the condenser, got through the expansion valve, then ingressed into the evaporator where the return chilled water was chilled down. The water vapour was then absorbed back to the lithium bromide solution in the absorber. By performing an energy balance,

$$Q_{cond} + Q_{ab} = Q_{gen} + Q_{evap} \quad (2)$$

The heat transfer inside the generator and the absorber were determined based on the log-mean-temperature-difference approach. For the condenser and the evaporator, the zone-model approach outlined by Lee and Lam [26] was adopted.

Dynamic system simulations were made for one year using a simulation time step of 6 minutes. The configuration of the GHE followed the one adopted by Lee and Lam [27] as summarized in Table 3 which was selected for the sole operation of the ground-source heat pump system for the entire building zone. Table 4 lists out the parameter

details of the absorption chiller, cooling water system, chilled water system, hot water system and supply air stream used in the absorption cooling part of the HRCS.

## 3. Comparative study with other renewable cooling systems

### *3.1 The associated cooling systems to be benchmarked*

To investigate clearly the energy-saving potential of HRCS, primary energy analysis was adopted. The comparative study included HRCS and the related cooling systems primarily driven by the corresponding renewable energy sources, these are:

- the solar absorption cooling system (SACS); and
- the ground-source heat pump system (GHPS).

Fig. 3 depicts the SACS, which was same as the HRCS except no ground-source radiant cooling was involved. Absorption chiller that was energized by the evacuated tube collectors provided chilled water to the supply air coil for building air-conditioning purpose. Fig. 4 illustrates the GHPS, which was electrically driven and made use of the ground source as heat sink for heat dissipation of the vapour compression refrigeration cycle. The chilled water generated from the heat pump was delivered to the supply air coil for air-conditioning provision of the building zone. In this case, the heat pump was actually functioning as a refrigeration machine. On the other hand, the energy performance of the conventional water-cooled vapour compression chiller system (VCCS) was also involved for benchmarking purpose, and its performance data was extracted from a previous study [28]. The entire comparative study was conducted on the same

basis of the building zone, the solar collectors and the borehole field for the respective cooling systems.

### *3.2 Performance parameters*

There are primarily three performance parameters involved in system evaluation and comparison. They are solar fraction, coefficient of performance and primary energy consumption. The yearly averaged zone temperature $T_{zone}$ and zone relative humidity $RH_{zone}$ will also be observed.

The effectiveness of the HRCS and SACS was represented by the solar fraction *SF* defined as:

$$SF = \frac{Solar \quad energy}{Solar \quad energy \quad + \quad auxiliary \quad energy} \tag{3}$$

*SF* measured the portion of the driving energy that came from the solar energy system, and a high *SF* means that a lower proportion of the driving energy was provided by the auxiliary energy source.

The performance of the cooling system was measured by the coefficient of performance (*COP*) defined as:

$$COP = \frac{Cooling \quad capacity}{Driving \quad energy} \tag{4}$$

About the driving energy, it depends on the type of cooling systems involved. For the absorption chiller of HRCS or SACS, the driving energy was the thermal input from solar energy system and/or auxiliary heater. For the compression chiller of GHPS or VCCS, the driving energy was solely the electricity from the city grid. In case of the HRCS, the cooling capacity included those from both the absorption chiller and the radiant panels.

The use of *COP* is limited since different kinds cannot be compared directly. A more general performance parameter, primary energy consumption, was therefore included. All parasitic energy consumptions from the pumps, the fans, the cooling tower and sundry items were accounted for. An energy efficiency of 33% was assumed for the electric power plant in relation to the primary energy input. The auxiliary gas heater was assumed to be run directly on primary energy with a combustion efficiency of 90%.

## 4. Results, discussions and further analysis

### *4.1 Year-round performances of various renewable and conventional cooling systems*

Table 5 compares the year-round-averaged performances of the various systems investigated. The primary energy consumptions of GHPS and VCCS were extracted from the previous studies of [27] and [28] respectively. All renewable cooling systems had better energy performance than the conventional VCCS. The HRCS with CC had year-round energy saving of 37%; the HRCS with PCB had 52%; the SACS had 31%; and the GHPS had 43%. Clearly, the HRCS with PCB was the best among the various renewable cooling systems in terms of primary energy consumption. Both HRCS's offered higher

year-round-averaged *SF's* and *COP's*, as well as better energy performance as compared to the SACS. Generally the use of CC yielded less satisfactory performance than PCB, which cohered with the findings from a previous study [29]. As the HRCS's employed the same GHE as that used in the GHPS, it was found that the HRCS with CC was less preferable since the resulting primary energy consumption was 10% higher. However, the HRCS with PCB could offer a primary energy saving of 15%. On the other hand, the SACS had 20% more energy consumption than the GHPS, showing that the driving source of solar energy could be less effective than that of ground-source for air-conditioning purpose.

From Table 5, it is noted that the two cases of HRCS have higher average $RH_{zone}$ compared to the other systems which fully relied on coil cooling. As mentioned in Section 2.1, the HRCS system offered temperature-control only in which both the supply air coil and the radiant panels would operate when the zone temperature was higher than the pre-set lower limit. To maximize the use of the radiant panels in order to minimize the use of the auxiliary heater, the ground-coupled radiant panel system operated in full capacity whenever it was energized. However, a modulating supply air coil valve was added and controlled by a proportional controller which regulated the chilled water supply flow to the supply air coil. In this regard, the dehumidification capacity of the supply air coil would be reduced, since the capacity of the solar-cooling part is sized according to the total system cooling requirement initially.

So far the analysis was based on dynamic simulation for one year only. As known, with an unbalanced annual borefield load, the ground temperature would change gradually. It might thus be argued whether the benefits of employing the hybrid

renewable cooling system could be maintained in the long run. To investigate, a two-year dynamic simulation was performed for the HRCS with CC. It was found that the year-round total primary energy consumption for the second year operation was only 0.4% higher than that for the first year operation. The main reason was that the borehole load per unit length adopted in the hybrid renewable cooling system was much lower than that used in the sole ground-source heat pump system. Hence, there was much more opportunity for the heat injected into the ground to be dispersed to the surrounding instead of accumulating around the borehole. In view of this, the current analysis which was based on one year simulation was considered appropriate.

### *4.2 Monthly performances of various renewable cooling systems*

Fig. 6 compares the monthly total primary energy consumptions for the various renewable cooling systems under study. From the annual profiles, the SACS had the highest primary energy demand in the summer period; next was the HRCS with CC; then the GHPS; and the HRCS with PCB had the least. The GHPS performed the best during the low-load period from December to March as compared to the other systems. The energy demand profiles for the SACS and the HRCS with CC were similar, with the peak demand in June, as well as the lower energy consumption in July than those in June and August. For the GHPS, the energy demand was the highest in July. In case of the HRCS with PCB, the peak demand occurred in August but the value was only slightly higher than those in June and July.

Fig. 7 shows the variation of the monthly-averaged *COP* for the three cooling systems with solar energy involved. The profiles of the HRCS's were substantially

different from that of the SACS. For the SACS, the *COP* was relatively constant, with only mild fluctuation over a year. This is because auxiliary heating would be called in whenever the heat supply from solar energy was not sufficient. However, for the HRCS, the *COP* was significantly higher during the peak-load season. This can be explained that the cooling capacity generated by the radiant panels increased largely and overrode the adverse effect from the lower performance of the absorption chiller during that period. As found in Fig. 7, the *COP* of the HRCS with CC was higher than that with PCB during the peak-load period. This seems not in line with the observations in the primary energy consumption profiles. However, the higher *COP* offered by the use of CC was due to the fact that the cooling capacity of CC was larger than that of PCB during the said period. Such higher cooling capacity was mainly contributed by radiative cooling rather than convective cooling, this reduced the capability of the HRCS with CC to lower the zone air temperature. Therefore, the absorption chiller had to operate at a longer time in order to maintain the zone temperature at the design level. This led to a higher primary energy consumption and correspondingly a lower *SF* as compared to those when PCB was employed.

### *4.3 HRCS with reduced capacity of absorption cooling part*

As discussed in Section 4.1, the HRCS with CC was less energy-efficient than the GHPS, although that with PCB was better. In addition, the HRCS's were not beneficial in view of greater complexity of system installation, the capital investment of HRCS may be 6 times higher than that of conventional system [30-32]. At first, the equipment design of the absorption cooling part of the HRCS was based on the SACS that could provide sufficient cooling for the building zone. As the radiant panels also provided cooling to

the building zone, there was potential for the HRCS to reduce the equipment size of the convective cooling system including the capacity of the absorption chiller, the supply air fan and the supply air coil. This would be highly beneficial as the parasitic energy consumption of the water pumps, the cooling tower and the supply air fan could be lowered. By reviewing the previous design data, the radiant panels provided a design cooling capacity of 10 kW. This was calculated based on the design borefield water flow and the possible temperature difference between the borefield water and the design zone temperature. Hence, the duty for the absorption chiller could be downsized to 19 kW. The loading allocation became about one-third from ground-source radiant cooling and two-third from solar-driven absorption cooling. The associated equipment of cooling water system, chilled water system and supply air stream of absorption cooling could then be reduced accordingly. Table 6 summarizes the corresponding parameter values for the absorption cooling part with the reduced capacity. The capacity of the solar energy and hot water system could be kept the same, and the solar thermal gain was maintained.

Table 7 shows the simulation results of the HRCS based on the reduced absorption cooling. Compared with Table 5, the *SF* was slightly decreased by 2.3% and 0.3% for HRCS with CC and HRCS with PCB respectively. As the cooling capacity of the absorption chiller was reduced, the corresponding running time for the chiller increased to a certain extent which caused the *SF* to drop subsequently. Meanwhile, the *COP* increased by 12.2% and 14.2% for HRCS with CC and HRCS with PCB respectively. This is because the ratio of the cooling capacity of the radiant panels to that for the absorption chiller increased. From Tables 5 and 7, the year-round-averaged zone conditions did not change much with PCB when the capacity of the absorption chiller was reduced. The daily temperature and relative humidity profiles of HRCS with PCB on the

hottest day in summer period are presented in Figs. 8 and 9 respectively. It is found that both the indoor temperature and the indoor relative humidity are close to the design conditions of 25.5°C and 60% respectively during the working hours. On the other hand, the energy performances of both HRCS were satisfactory in reduction of total primary energy consumption, ranging from 18.0% to 43.8% when compared with the GHPS. In this connection, both HRCS's became technically feasible among the renewable cooling systems under study. Now, it could even reach 53.3% and 68.0% energy saving when benchmarked against the SACS and the VCCS respectively. This indicates the design effectiveness of the HRCS and its hybrid use of renewable energy sources. In fact, the ground temperature with sufficient depth was stably maintained at a level which allowed the circulating water to be cooled to the temperature required by the radiant panels. As no additional mechanical cooling device was needed, high energy efficiency could be achieved, which helped decrease the overall primary energy consumption of the HRCS.

## 5. Conclusion

In general, renewable energy sources are separately considered to provide air-conditioning for buildings, like the solar sorption systems or the geothermal heat pump systems. Through the paradigm of renewable cooling and hybrid association of solar energy and ground source, the idea of HRCS was generated for principal building air-conditioning in the hot and humid climate. Solar energy was used to drive the absorption refrigeration cycle, while ground source was applied for the radiant cooling. In a typical office building with subtropical climate, the appropriate sharing of total cooling capacity was investigated, and it was two-third from the solar-driven part and one-third from the

ground-source part. The HRCS was found to have a remarkable energy performance with PCB in radiant cooling, its year-round primary energy consumption could be 43.8%, 53.3% and 68.0% lower than that of the sole ground-based GHPS, the sole solar-driven SACS and the conventional electrical VCCS respectively.

In the annual profiles, the monthly system performances of HRCS were observed in different seasons. Throughout the year, the HRCS with PCB could maintain better energy performance and good COP, showing that it had more effective system design as a whole. In the summer time, even the HRCS with CC could provide higher COP than that with PCB, its primary energy consumption was also more. Since CC had higher radiative load ratio, it demanded more operation of absorption chiller to maintain the required design indoor conditions. In a hybrid system design, it is paramount to understand the contributions from key components in a holistic and year-round approach. In pursuit of their appropriate capacity sizing, the merits in hybrid system design could be fully facilitated.

For renewable cooling, there is still room of involvement of renewable source. For instance, bioenergy can be used for auxiliary heating of solar absorption cooling, this would get rid of the primary energy consumption from natural gas or any fossil fuel. In fact, continuous advancement of biofuel technology would promote its feasibility and availability in supporting renewable cooling. Consequently, development of renewable cooling would be leading towards low-carbon air-conditioning for building application. This is apparently beneficial to the deployment of sustainable technology in the hot and humid cities.

**Acknowledgement**

This work described in this paper is fully supported by a grant from the Research Grants Council of the Hong Kong Special Administrative Region, China (Project No. CityU 123812).

**References**

[1] *Solar Heating and Cooling Programme*, International Energy Agency, website: http://www.iea-shc.org

[2] *Solar air conditioning*, Solar Heating and Cooling Program of the International Energy Agency: Task 25 – Solar Assisted Air Conditioning of Buildings, 2004.

[3] Wang RZ, Ge TS, Chen CJ, Ma Q, Xiong ZQ. Solar sorption cooling systems for residential applications: Options and guidelines. *International Journal of Refrigeration* 2009;32:638-60.

[4] Eicker U. *Solar Technologies for Buildings*. Chichestor: Wiley, 2003.

[5] Henning H-M. *Solar-Assisted Air-Conditioning in Buildings, A Handbook for Planners*. Springer-Verlag Wien New York, 2004.

[6] Wang RZ, Zhai XQ. Development of solar thermal technologies in China. *Energy* 2010;35:4407-16.

[7] *Renewables for Heating and Cooling, Untapped Potential. International Energy Agency*, IEA Publications, November 2007.

[8] Verbruggen A, Fischedick M, Moomaw W, Weir T, Nadai A, Nilsson LJ, Nyboer

J, Sathaye J. Renewable energy costs, potentials, barriers: Conceptual issues. *Energy Policy* 2010;38:850-61.

[9] Seyboth K, Beurskens L, Langniss O, Sims REH. Recognising the potential for renewable energy heating and cooling. *Energy Policy* 2008;36:2460-3.

[10] *Key issues for Renewable Heat in Europe K4RES-H*. European Renewable Energy Council, website: http://www.erec.org/projects/finalised-projects/k4-res-h.html, last accessed on 10 December 2013.

[11] Georgiev A, Busso A, Roth P. Shallow borehole heat exchanger: Response test and charging-discharging test with solar collectors. *Renewable Energy* 2006;31(7):971-85.

[12] Ozgener O, Hepbasli A. Experimental performance analysis of a solar assisted ground-source heat pump greenhouse heating system. *Energy and Buildings* 2005;37(1):101-10.

[13] Wang F, Zheng MY, Shao JP, Li ZJ. Simulation of embedded heat exchangers of solar aided ground source heat pump system. *Journal of Central South University of Technology* 2008;15:261-6.

[14] Kim W, Choi J, Cho H. Performance analysis of hybrid solar-geothermal CO2 heat pump system for residential building. *Renewable Energy* 2013;50:596-604.

[15] Fong KF, Chow TT, Lee CK, Lin Z, Chan LS. Comparative study of different solar cooling systems for buildings in subtropical city. *Solar Energy* 2010;84(2)227-44.

[16] *TRNSYS 16, a TRaNsient SYstem Simulation program,* the Solar Energy Laboratory, University of Wisconsin-Madison, 2006.

[17] *TESS Library Documentation*, Thermal Energy System Specialists, 2006.

[18] *Guidelines on Performance-based Building Energy Code*, EMSD, Hong Kong SAR Government, http://www.emsd.gov.hk/emsd/e_download/pee/PBBEC_Guidelines_2007.pdf , last accessed on 10 December 2013.

[19] Chan ALS, Chow TT, Fong SKF, Lin JZ. Generation of a typical meteorological year for Hong Kong. *Energy Conversion and Management* 2006;47:87-96.

[20] *TRNSYS 16, Volume 6, Multizone Building modeling with Type56 and TRNBuild*. The Solar Energy Laboratory, University of Wisconsin-Madison, November 2005.

[21] Carrier, Chilled Beams Product Selection Data, model 36CB QPBA-420. http://www.ahi-carrier.com.au/upload/data/Products-%20Commercial/36CB-QP%20passive.pdf, last accessed on 10 December 2013.

[22] Hochschul Rapperswil of Switzerland, Test Report No. 264, 1997.

[23] Lee CK and Lam HN. Computer simulation of borehole ground heat exchangers for geothermal heat pump systems. *Renewable Energy* 2008;33(6):1286-96.

[24] Hellstrom G. *Ground Heat Storage. Thermal Analysis of Duct Storage Systems: part I theory*, Doctoral Thesis, Department of Mathematical Physics, University of Lund, Sweden, 1991.

[25] Fong KF, Lee CK and Chow TT. Comparative study of solar cooling systems with building-integrated solar collectors for use in sub-tropical regions like Hong Kong. *Applied Energy* 2012;90(1):189-95.

[26] Lee CK and Lam HN. Computer simulation of ground-coupled liquid desiccant air conditioner for sub-tropical regions. *International Journal of Thermal Sciences* 2009;48(12): 2365-74.

[27] Lee CK and Lam HN. Application potential of ground-coupled heat pumps for multi-storey office building in Hong Kong. *Proceedings of Building Simulation 2011*, Sydney, paper no. 1137.

[28] Fong KF, Lee CK, Lin Z, Chow TT and Chan LS. Application potential of solar air-conditioning systems for displacement ventilation. *Energy and Buildings* 2011;43(9):2068-76.

[29] Fong KF, Lee CK, Chow TT, Lin Z and Chan LS. Solar hybrid air-conditioning system for high temperature cooling in subtropical city. *Renewable Energy* 2010;35(11):2439-51.

[30] *Hong Kong Report – Quarterly Construction Cost Update*, Rider Levett Bucknall, March 2011.

[31] Lau KF and Suen MT. Geothermal heat pump air-conditioning system for the Hong Kong International Wetland Park. *Proceedings of Shandong-Hong Kong Joint Symposium 2003*, Qingdao, China, 17-18 October 2003.

[32] Jakob U. Commercialising of thermal powered refrigeration, SIRAC – London Network Meeting, University College London, U.K., October 2009.

**Figures captions**

Fig. 1. Schematic diagram of hybrid renewable cooling system for building application.

Fig. 2. Ground discretization scheme adopted by Lee and Lam [23].

Fig. 3. Schematic diagram of a single-effect lithium bromide absorption chiller [25].

Fig. 4. Schematic diagram of solar absorption cooling system.

Fig. 5. Schematic diagram of ground-source heat pump system for building cooling.

Fig. 6. Comparison of the monthly total primary energy consumptions for the various renewable cooling systems.

Fig. 7. Comparison of the monthly-averaged *COP* for the various solar cooling systems.

Fig. 8. Daily temperature profile of the HRCS with PCB and reduced capacity of absorption cooling part on the hottest day (T_amb: Ambient temperature; T_zone: Zone temperature; T_design: Indoor design temperature).

Fig. 9. Daily relative humidity profile of the HRCS with PCB and reduced capacity of absorption cooling part on the hottest day (RH_amb: Ambient relative humidity; RH_zone: Zone relative humidity; RH_design: Indoor design relative humidity).

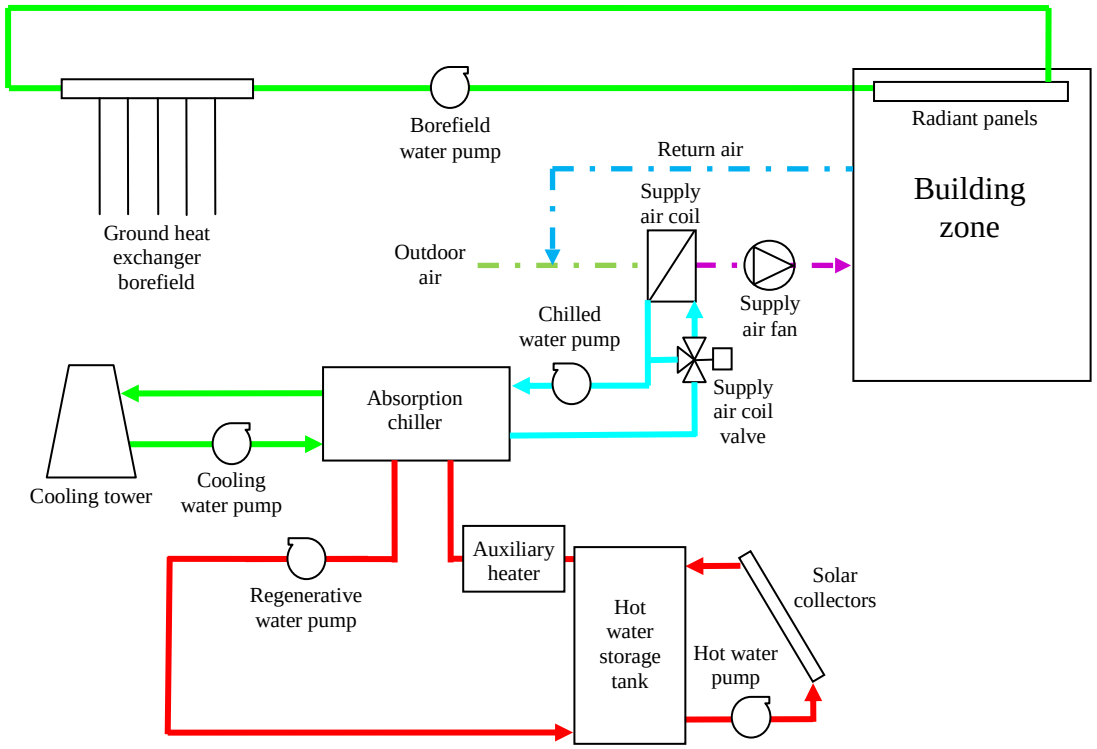


Fig. 1. Schematic diagram of hybrid renewable cooling system for building application.

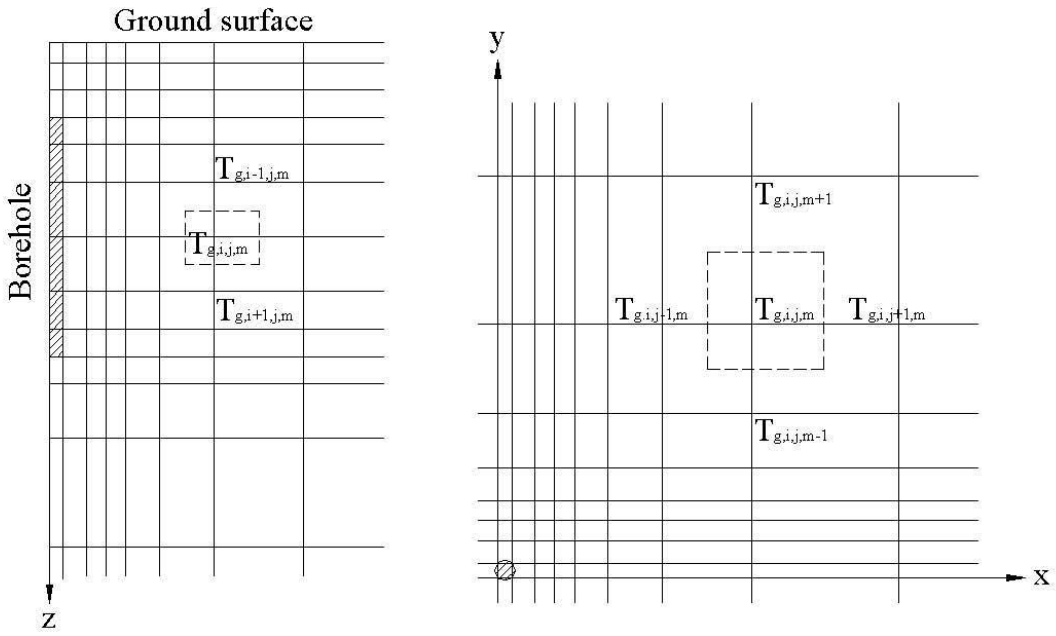


Fig. 2. Ground discretization scheme adopted by Lee and Lam [23].

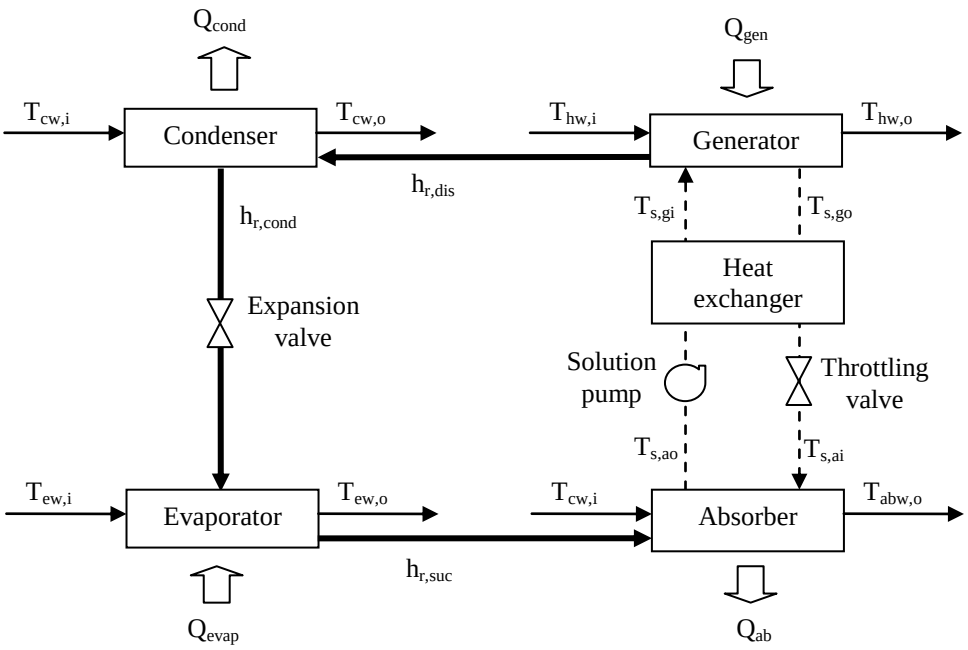


Fig. 3. Schematic diagram of a single-effect lithium bromide absorption chiller [25].

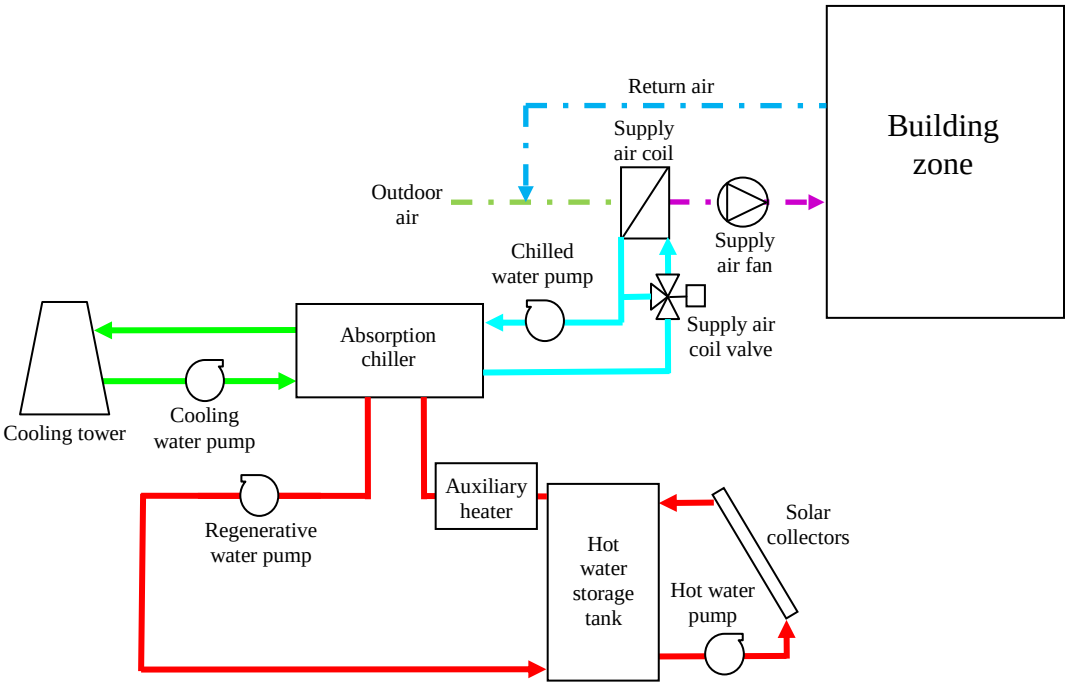


Fig. 4. Schematic diagram of solar absorption cooling system.

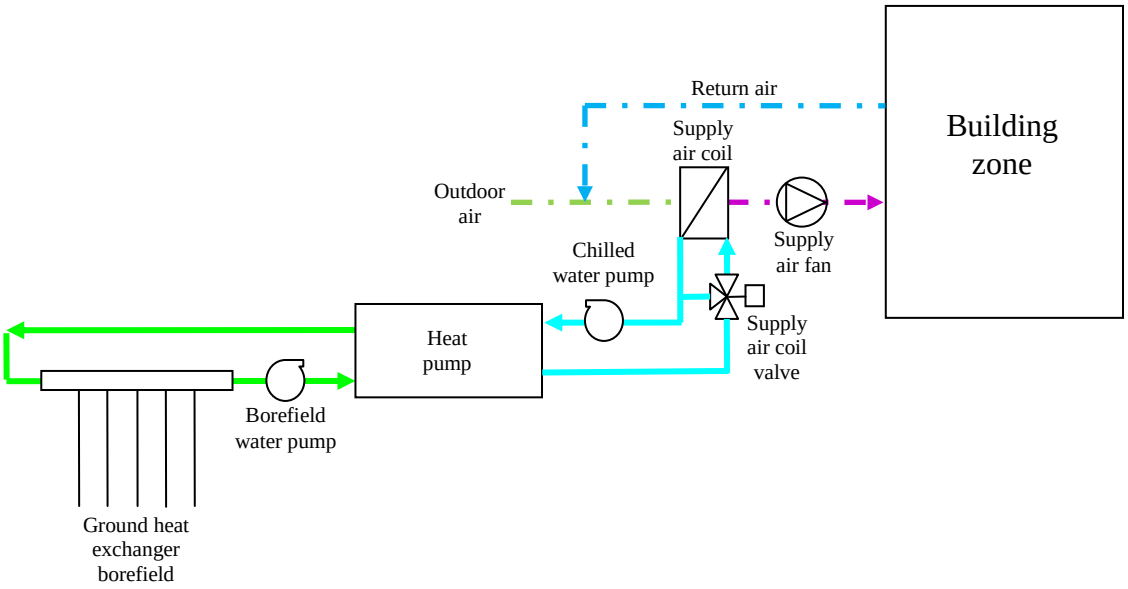


Fig. 5. Schematic diagram of ground-source heat pump system for building cooling.

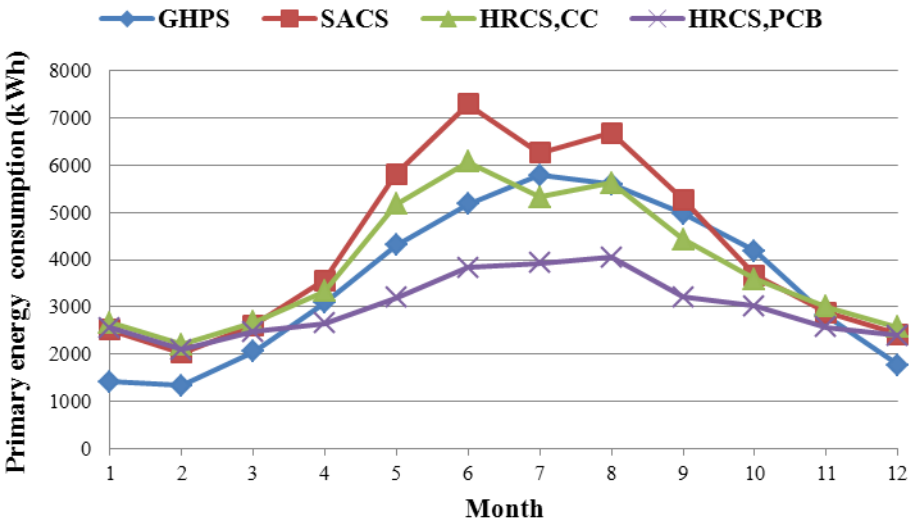


Fig. 6. Comparison of the monthly total primary energy consumptions for the various renewable cooling systems.

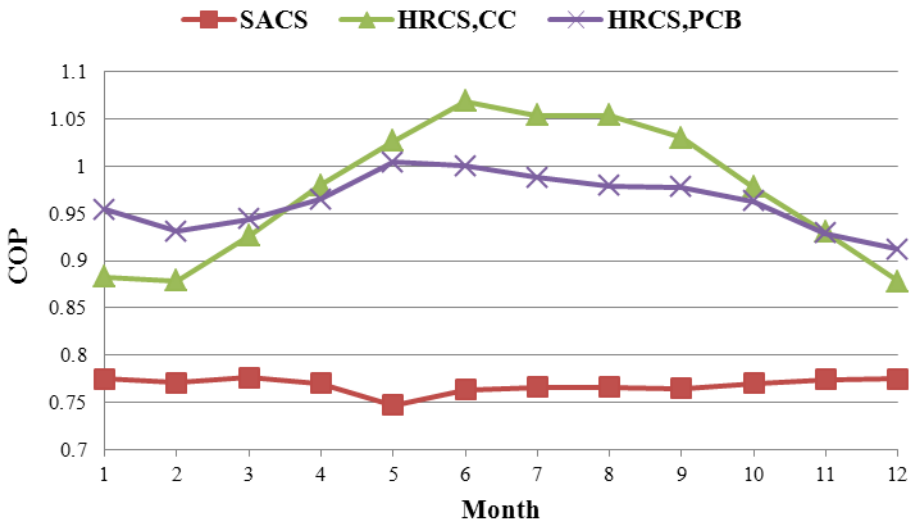


Fig. 7. Comparison of the monthly-averaged *COP* for the various solar cooling systems.

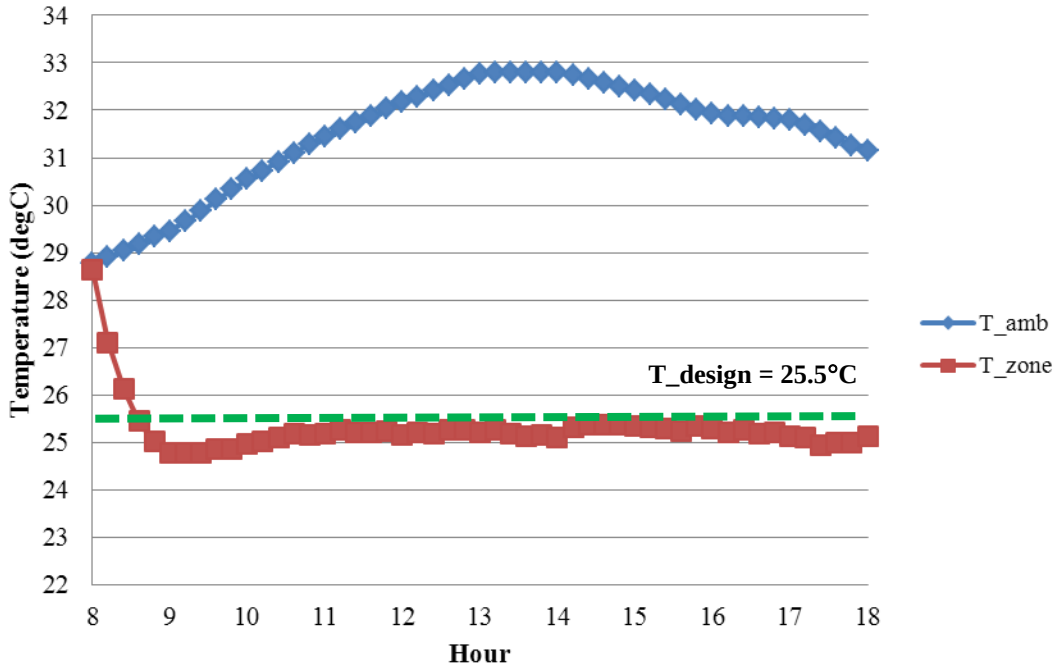


Fig. 8. Daily temperature profile of the HRCS with PCB and reduced capacity of absorption cooling part on the hottest day (T_amb: Ambient temperature; T_zone: Zone temperature; T_design: Indoor design temperature).

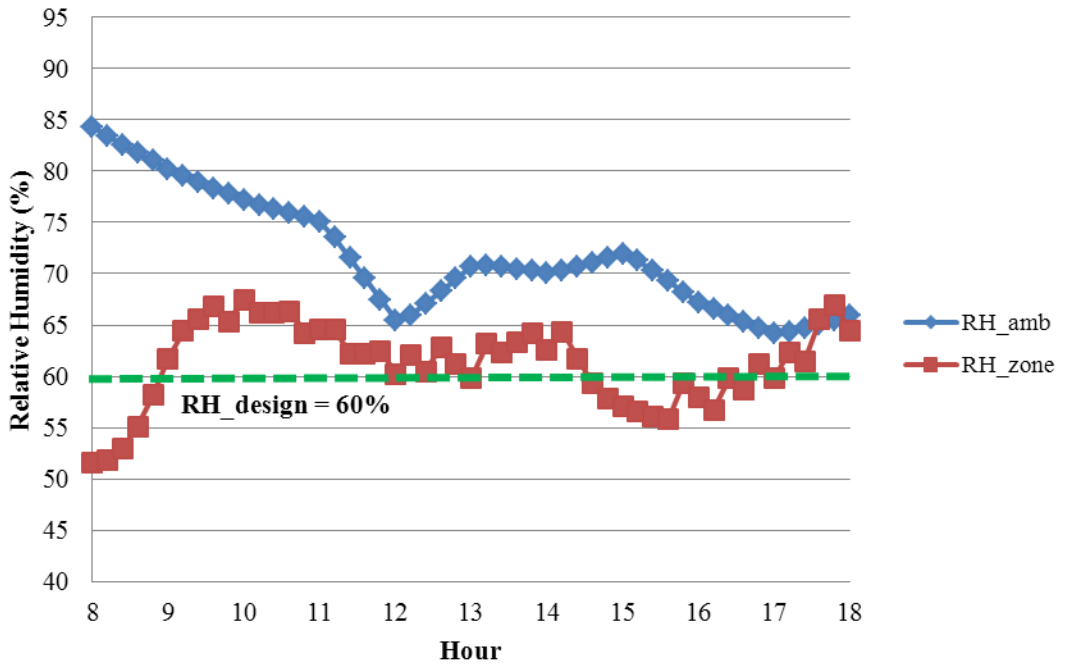


Fig. 9. Daily relative humidity profile of the HRCS with PCB and reduced capacity of absorption cooling part on the hottest day (RH_amb: Ambient relative humidity; RH_zone: Zone relative humidity; RH_design: Indoor design relative humidity).

**Table captions**

Table 1. Constructional characteristics and parameter values of typical office building under study.

| Parameter | Value |
|---|---|
| Length and width of typical floor (m × m) | 14 × 14 |
| Floor-to-floor height (m) | 3.6 |
| Number of storey | 1 |
| U-value of external wall (reinforced concrete completed with external plastering and internal plastering) ($W \cdot m^{-2} \cdot K^{-1}$) | 2.73 |
| U-value of window (single glazing) ($W \cdot m^{-2} \cdot K^{-1}$) | 5.68 |
| U-value of flat roof (reinforced concrete completed with thermal insulation and water-proofing layer) ($W \cdot m^{-2} \cdot K^{-1}$) | 0.39 |
| Shading coefficient of window | 0.25 |
| Window to wall ratio | 0.5 |

Table 2. Monthly averages of the key meteorological data of Hong Kong.

| | Dry bulb temperature (°C) | Dew point temperature (°C) | Total solar radiation ($MJ \cdot m^{-2} \cdot day^{-1}$) | Wind speed ($m \cdot s^{-1}$) |
|---|---|---|---|---|
| January | 16.12 | 11.49 | 9.14 | 2.78 |
| February | 16.30 | 12.80 | 9.69 | 3.65 |
| March | 19.03 | 15.85 | 10.46 | 2.89 |
| April | 22.59 | 19.71 | 12.13 | 3.41 |
| May | 26.07 | 22.55 | 13.21 | 2.55 |
| June | 27.92 | 25.00 | 13.88 | 3.34 |
| July | 28.85 | 24.87 | 17.73 | 3.02 |
| August | 28.44 | 24.85 | 15.59 | 2.84 |
| September | 27.54 | 23.80 | 14.40 | 3.68 |
| October | 25.32 | 19.79 | 14.57 | 3.12 |
| November | 21.53 | 15.35 | 12.46 | 2.94 |
| December | 17.11 | 10.50 | 11.01 | 2.86 |

Table 3. Parameter values of the ground heat exchanger borefield.

| Parameter | Value |
|---|---|
| Borefield configuration | 3 x 3 |
| Borehole separation (m) | 4.5 |
| Borehole radius (m) | 0.055 |
| Insulated length of borehole (m) | 5 |
| Effective length of borehole (m) | 110 |
| Number of U-tube inside each borehole | 1 |
| Tube inner radius (m) | 0.013 |
| Tube outer radius (m) | 0.016 |
| Distance of tube centre from borehole centre (m) | 0.03 |
| Ground thermal conductivity ($W \cdot m^{-1} \cdot K^{-1}$) | 3.5 |
| Ground volumetric heat capacity ($kJ \cdot m^{-3} \cdot K^{-1}$) | 2160 |
| Borefield water specific heat capacity ($kJ \cdot kg^{-3} \cdot K^{-1}$) | 4.19 |
| Borefield water density ($kg \cdot m^{-3}$) | 1000 |
| Borefield water thermal conductivity ($W \cdot m^{-1} \cdot K^{-1}$) | 0.614 |
| Borefield water dynamic viscosity ($kg \cdot m^{-1} \cdot s^{-1}$) | 0.00086 |
| Pipe thermal conductivity ($W \cdot m^{-1} \cdot K^{-1}$) | 0.4 |
| Grout thermal conductivity ($W \cdot m^{-1} \cdot K^{-1}$) | 1.3 |
| Total borefield water mass flow rate ($kg \cdot s^{-1}$) | 1.5 |
| Borefield water pump efficiency | 60% |

Table 4. Parameter values of absorption cooling part of the HRCS.

| Parameter | Value |
|---|---|
| **Absorption Chiller** | |
| Regenerative water mass flow rate ($kg \cdot s^{-1}$) | 2.0 |
| Condenser water mass flow rate ($kg \cdot s^{-1}$) | 1.6 |
| Absorber water mass flow rate ($kg \cdot s^{-1}$) | 2.0 |
| Chilled water mass flow rate ($kg \cdot s^{-1}$) | 1.4 |
| Specific heat capacity of liquid water ($kJ \cdot kg^{-1} \cdot K^{-1}$) | 4.19 |
| Overall heat transfer value of generator ($kW \cdot K^{-1}$) | 4.5 |
| Overall heat transfer value of absorber ($kW \cdot K^{-1}$) | 4.5 |
| Overall heat transfer value of solution-to-solution heat exchanger ($kW \cdot K^{-1}$) | 1.0 |
| Overall heat transfer value of condenser ($kW \cdot K^{-1}$) | 4.8 |
| Overall heat transfer value of evaporator ($kW \cdot K^{-1}$) | 4.3 |
| Degree of superheat at evaporator outlet ($^{o}C$) | 5.0 |
| Solution volume flow rate at absorber outlet ($l \cdot s^{-1}$) | 0.1 |
| **Cooling water system** | |
| Cooling tower air volume flow rate ($m^3 \cdot s^{-1}$) | 2.22 |
| Cooling tower fan head (Pa) | 200 |
| Cooling tower fan efficiency | 65% |
| Cooling water pipe (Diameter x length) (mm x m) | 80 x 100 |
| Cooling water pump head (kPa) | 116 |
| Cooling water pump efficiency | 60% |
| **Chilled water system** | |
| Chilled water pipe (Diameter x length) (mm x m) | 50 x 100 |
| Chilled water pump head (kPa) | 120 |
| Chilled water pump efficiency | 60% |
| **Hot water system** | |
| Hot water mass flow rate ($kg \cdot s^{-1}$) | 2.0 |
| Hot water pipe (Diameter x length) (mm x m) | 50 x 100 |
| Hot water pump head (kPa) | 60 |
| Hot water pump efficiency | 60% |
| Regenerative water pipe (Diameter x length) (mm x m) | 50 x 10 |
| Regenerative water pump head (kPa) | 72 |
| Regenerative water pump efficiency | 60 |
| **Supply air stream** | |
| Supply air mass flow rate ($kg \cdot s^{-1}$) | 2.15 |

| | |
|---|---|
| Supply air fan head (Pa) | 750 |
| Supply air fan efficiency | 70% |
| Face area of supply air coil ($m^2$) | 0.9 |

Table 5. Comparison of year-round performances of various systems.

| System | *SF* | *COP* | Primary energy consumption (kWh) | $T_{zone}$ ($^{o}$C) | $RH_{zone}$ (%) |
|---|---|---|---|---|---|
| HRCS,CC | 0.876 | 1.018 | 46,637 | 24.7 | 62.8 |
| HRCS,PCB | 0.962 | 0.980 | 35,955 | 24.4 | 69.5 |
| SACS | 0.805 | 0.765 | 50,996 | 24.8 | 58.7 |
| GHPS | NA | NA | 42,394 [27] | NA | NA |
| VCCS | NA | 3.195 | 74,431 [28] | 24.8 | 58.9 |

Remarks: “NA” means “not applicable” or “not available”.

Table 6. Parameter values of the HRCS with absorption cooling at reduced capacity.

| Parameter | Value |
|---|---|
| **Absorption Chiller** | |
| Regenerative water mass flow rate ($kg \cdot s^{-1}$) | 1.3 |
| Condenser water mass flow rate ($kg \cdot s^{-1}$) | 1.0 |
| Absorber water mass flow rate ($kg \cdot s^{-1}$) | 1.3 |
| Chilled water mass flow rate ($kg \cdot s^{-1}$) | 0.9 |
| Specific heat capacity of liquid water ($kJ \cdot kg^{-1} \cdot K^{-1}$) | 4.19 |
| Overall heat transfer value of generator ($kW \cdot K^{-1}$) | 3.0 |
| Overall heat transfer value of absorber ($kW \cdot K^{-1}$) | 3.0 |
| Overall heat transfer value of solution-to-solution heat exchanger ($kW \cdot K^{-1}$) | 0.6 |
| Overall heat transfer value of condenser ($kW \cdot K^{-1}$) | 3.0 |
| Overall heat transfer value of evaporator ($kW \cdot K^{-1}$) | 2.5 |
| Degree of superheat at evaporator outlet ($^{o}C$) | 5.0 |
| Solution volume flow rate at absorber outlet ($l \cdot s^{-1}$) | 0.07 |
| **Cooling water system** | |
| Cooling tower air volume flow rate ($m^3 \cdot s^{-1}$) | 1.75 |
| Cooling tower fan head (Pa) | 200 |
| Cooling tower fan efficiency | 65% |
| Cooling water pipe (Diameter x length) (mm x m) | 65 x 100 |
| Cooling water pump head (kPa) | 120 |
| Cooling water pump efficiency | 60% |
| **Chilled water system** | |
| Chilled water pipe (Diameter x length) (mm x m) | 40 x 100 |
| Chilled water pump head (kPa) | 130 |
| Chilled water pump efficiency | 60% |
| **Supply air stream** | |
| Supply air mass flow rate ($kg \cdot s^{-1}$) | 0.97 |
| Supply air fan head (Pa) | 750 |
| Supply air fan efficiency | 70% |
| Face area of supply air coil ($m^2$) | 0.4 |

Table 7. Year-round performances of the HRCS with absorption cooling at reduced capacity.

| System | *SF* | *COP* | Primary energy consumption (kWh) | $T_{zone}$ ($^{o}$C) | $RH_{zone}$ (%) |
|---|---|---|---|---|---|
| HRCS,CC | 0.856 | 1.142 | 34,743 | 25.4 | 55.9 |
| HRCS,PCB | 0.959 | 1.119 | 23,813 | 24.5 | 66.8 |